

Facile two-step Electrodeposition Synthesis of CuO Nanowires for Ultrasensitive Non-Enzymatic Sensing of Glucose

Di Zhang ^{1,†}, Yuyun Wei ^{2,†}, Meidan Zhao², Hong Wang², Qing Xia², Yuxin Fang^{2,*}

¹ College of Pharmaceutical Engineering of Traditional Chinese Medicine, Tianjin University of Traditional Chinese Medicine, Tianjin 301617, PR China

² Research Center of Experimental Acupuncture Science, College of Acumox and Tuina, Tianjin University of Traditional Chinese Medicine, Tianjin 301617, PR China

*E-mail: meng99_2006@126.com

†These authors contributed equally.

Received: 9 July 2019 / Accepted: 17 September 2019 / Published: 29 October 2019

In this manuscript, well-defined copper(II) oxide nanowires (CuO NWs) structures were successfully synthesized by simple, template- and surfactant-free two-step electrodeposition method. The obtained CuO NWs were investigated using field emission scanning electron microscopy (FESEM) and X-ray photoelectron spectroscopy (XPS). The electrochemical properties of the CuO NWs modified glassy carbon (CuO NWs/GC) electrode towards nonenzymatic detection of glucose (Glc) under alkaline conditions were studied by cyclic voltammetry (CV) and chronoamperometry. Excellent electroreduction activity of CuO NWs towards Glc was observed. The CuO NWs/GC sensor was characterized by the wide linear range for Glc (0.0125-4.29 mM), high sensitivity ($759.86 \mu\text{A mM}^{-1} \text{cm}^{-2}$), short response time (4s) and the low limit of detection (LOD = $4.17 \mu\text{M}$). Moreover, the sensor showed good reproducibility, anti-interferant ability and long-term stability. Hence it suggests a potential applicability of CuO NWs/GC as a sensor for nonenzymatic detection and quantification of glucose.

Keywords: electrodeposition; CuO nanowires; glucose sensor; non-enzyme

1. INTRODUCTION

Analytical determination of glucose (Glc) is applied in various aspects of daily life [1-2]. Since the discovery of enzymatic detection of Glc in 1965, various sensors have been developed [3-4]. Enzymatic Glc sensors are widely applied, owing to high selectivity and fast response, but low chemical instability, high cost, stringent storage conditions etc. [5-7] are the limiting factors for this type of sensors. To overcome these issues, great research efforts have been invested to develop the effective, enzyme-free sensors. The principle of nonenzymatic Glc sensors is to directly oxidize Glc at the surface of electrode using various electrocatalysts and monitor the corresponding electrocurrent.

Following the recent progress in nanotechnology, various nanomaterials such as Au, Pt, Cu, Ag, and their alloys or oxides have been studied as catalysts for nonenzymatic Glc sensors [8-11]. Among them, copper(II) oxide (CuO) appeared as the most promising candidate for nonenzymatic Glc sensing owing to high catalytic activity, low overpotential for electron-transfer [12-13] and nontoxic nature. It is well-known that the shape and dimensions of nanomaterials strongly influence their properties. It has been shown that the morphology of metal oxides affect the electrochemical performance of Glc sensors [14-15]. Different CuO nanostructures such as nanoparticles [16], nanosheets [17], nanoflowers [18], and nanocubes [19] vary in specific surface area (SA), which is a determining factor for electron- and mass transport efficiency. To date, different CuO nanoarchitectures have been utilized as sensors. Zhang et al. produced nonenzymatic Glc sensors based on petal-like CuO nanostructures by a wet-chemistry route [20]. Zhao and co-workers used the functionalized PDDA-graphene/CuO nanocomposites for the modification of electrodes [21]. Yuan et al. successfully prepared 3D CuO nanosheets wrapped nanofilms grown on Cu substrate and tested as Glc sensor [22]. It is widely accepted that the synthetic procedure highly influences the morphology and properties of CuO nanostructures. However, most previous attempts are limited by complex fabrication and the prepared sensors exhibit a poor linear detection range.

This study reports a successful, template- and surfactant-free synthesis of well-defined copper oxide nanowires (CuO NWs) structures via two-step electrodeposition. Electrodeposition allows the production of broad range of nanomaterials with high SA, under highly controlled experimental conditions. The CuO NWs were electrodeposited on a surface of GC electrode, without using any additional fixation technique. The structural and morphological properties of a modified GC electrode was thoroughly studied. The obtained material exhibited good electrochemical properties, indicating a promising application as an electrocatalyst for Glc sensing.

2. EXPERIMENTAL

2.1. Reagents and materials

Glucose, copper(II) chloride dihydrate ($\text{CuCl}_2 \cdot 2\text{H}_2\text{O}$), sodium hydroxide (NaOH) and potassium chloride (KCl) were purchased from Tianjin Chemical Reagent Co (China). Dopamine (DA), ascorbic acid (AA) and uric acid (UA) were ordered from Sigma–Aldrich (USA). Analytical grade solutions and doubly distilled water were used in all experiments. The experiments were done at r.t., approx. 25 °C.

2.2. Apparatus and electrochemical measurement

The three-electrode system comprising of CuO NW/GC (3 mm in diameter) as a working electrode, reference Ag/AgCl electrode filled with saturated KCl and 1 mm Pt wire as a counter electrode was used for electrochemical measurements. All experiments were conducted on a 283 Potentiostat–Galvanostat workstation (EG & G PARC with M270 software).

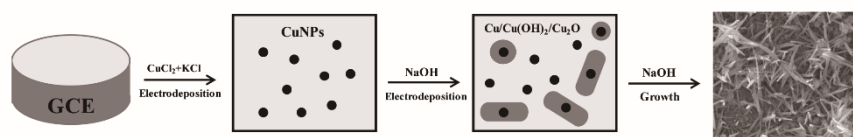
Steady-state amperometric experiments were conducted in 0.1M NaOH under the gentle magnetic stirring, where electrode potential was fixed at 0.55 V. Field emission SEM (FESEM) images were acquired using Nova NanoSEM 430 instrument (FEI, USA) equipped with an EDX accessory. The atomic composition and corresponding electronic states were studied by XPS (Axis Ultra) with Al-K α X-ray source.

2.3. Growth of CuO NWs modified GC electrode

The GC electrode was prepared for modification by polishing with Al₂O₃ slurry twice (first with 0.3 and then with 0.05 μm particle size), followed by cleaning with EtOH and water in ultrasonic bath to eliminate physically adsorbed molecules from the surface. The growth of CuO NWs on GC electrode was achieved via a facile two-step electrodeposition procedure. In the first step, Cu film was electrodeposited on GC surface keeping the potential of 0.1M KCl solution containing 10 mM CuCl₂ at -1.0 V for 10 min. Afterward, the electrode was rinsed with H₂O and dried using N₂. In the second step, Cu nanowires were prepared by placing the Cu film-modified GC electrode into 0.1M NaOH and running the 22 cycles of potential scan in the range from -0.5 to 0.3 V at the scan rate of 50 mV s⁻¹. The O₂ was removed from all solutions by purging the high-purity N₂ for at least 30 min, followed by a gentle blowing N₂ over the surface to maintain oxygen-free conditions during the measurements.

3. RESULTS AND DISCUSSION

3.1. Morphology and structural characterization of CuO NWs



Scheme 1. The schematic representation of two-step electrodeposition procedure leading to CuO NWs.

The plausible mechanism of the synthesis of CuO NWs is illustrated in Scheme 1. Briefly, the reduction of copper (II) chloride by EG generates Cu nanoparticles in the reaction mixture. Assisted by an alkaline environment, Cu is converted into large, rod-shaped CuO nanoparticles, which might grow further into nanowires. The large remaining surface area is highly attractive towards new Cu atoms, promoting the formation of nanowires [23]. Further research directed toward the exact mechanism of CuO NWs formation is in progress in our laboratories.

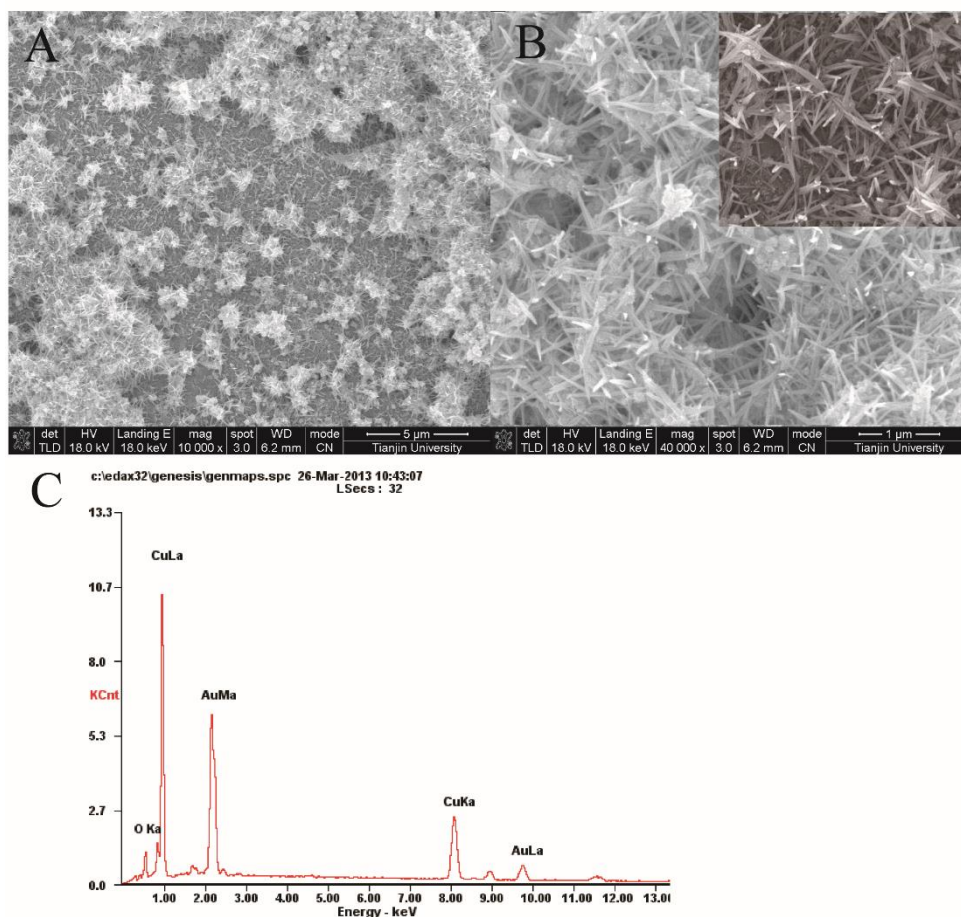


Figure 1. FESEM images of CuO NWs recorded with (A) low and (B) high magnification; (C) EDX spectrum of CuO NWs.

The surface morphology of CuO NWs product was characterized by FESEM, indicating the wire-shaped CuO nanoparticles (Fig. 1A and B). By growing into random directions, NWs created a network structure on the surface of GC electrode, with NWs length up to several hundred nanometers. The resulting modified GC electrode had significantly larger SA providing better mass transport at the surface, leading to the improved electrochemical performance.

Additionally, the EDX analysis confirm the presence of the pure copper and oxygen atoms in CuO NWs (Fig. 1C), while Au signals observed most likely originate from the substrate.

The chemical composition and oxidation state of Cu at the surface of CuO NWs was examined by XPS (Fig. 2). The presence of Cu at the surface was indicated by two sharp peaks of Cu 2p region (Fig. 2A) at the binding energies (E_b) of 932 eV and 951.9 eV, associated with Cu 2p^{3/2} and Cu 2p^{1/2} electrons [17, 24]. The Cu²⁺ oxidation state was revealed by shake-up satellite peaks at $E_b = 941.4$ eV and $E_b = 959.8$ eV [25-28]. The high resolution XPS spectrum of O 1s is given in Fig. 2B. The peaks at $E_b = 529.3$ eV and $E_b = 530.7$ eV can be associated with the oxygen in CuO lattice (Cu-O) and oxygen in H₂O (-OH) [29].

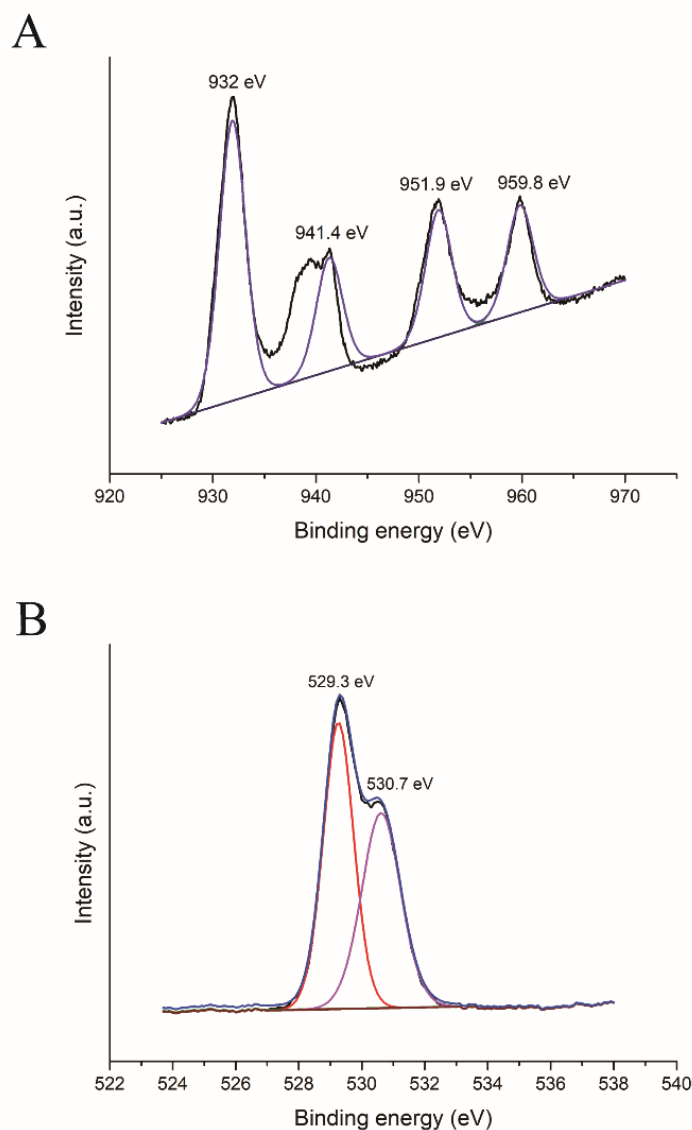


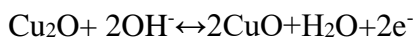
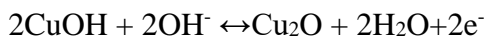
Figure 2. XPS survey spectrum of CuO NWs: High-resolution Cu 2p (A) and O 1s (B).

3.2. Electrochemical characterization and practical aspects of CuO NW/GC electrode

3.2.1. Electrochemical behavior of CuO NW/GC electrode

Cyclic voltammetry (CV) was utilized for studying the redox properties of CuO nanowires formed at the surface of GC. According to Fig. 3 (A), the Cu film modified GC electrode in 0.1M NaOH showed two anodic peaks (peak A₁ and A₂) and two cathodic peaks (peak C₁ and C₂) between -0.9 V to 0.3 V potential range. The A₁ and A₂ peaks detected at -0.35 V and -0.05 V originated from oxidation of Cu⁰ to Cu⁺ and further into Cu²⁺, while peaks C₁ and C₂ at -0.4 V and -0.8V represented the corresponding reductions of Cu²⁺ to Cu⁺ and from Cu⁺ to Cu⁰. Repeated cycles of CV lead to the decrease in intensity of redox peaks, suggesting the formation of CuO during the experiment (data not shown).

Similar behavior is already reported [30]. The tentative electrodeposition mechanism is represented by the following chemical equations:



As a valuable technique for studying surface properties and charge transfer characteristics of modified GC material, CV was performed in the presence of ferricyanide ions.

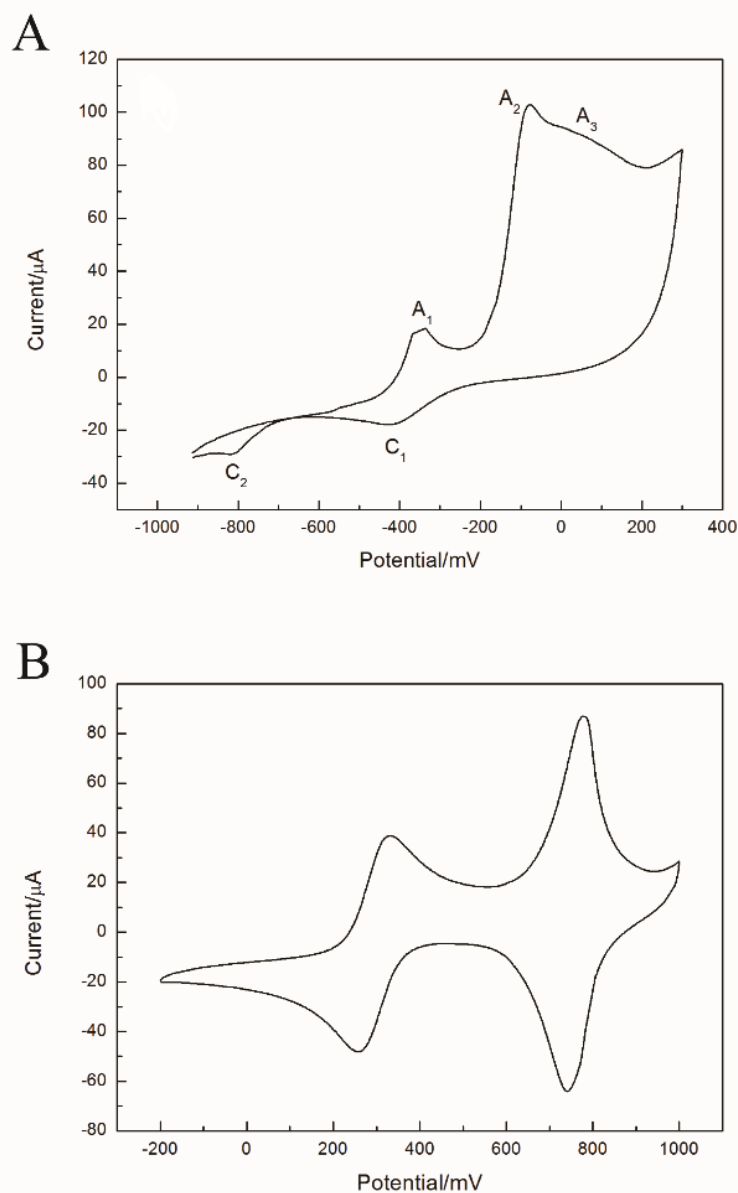
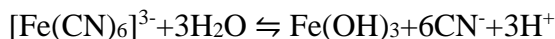


Figure 3. The cyclic voltammograms of (A) Cu/GC electrode in 0.1M NaOH, (B) CuO NWs/GC electrode in 0.1 M KCl solution containing 5 mM $\text{K}_3[\text{Fe}(\text{CN})_6]$.

The typical CV of the CuO NW/GC electrode in 0.1 M KCl mixed with 5 mM $[\text{Fe}(\text{CN})_6]^{3-}$ is represented in Fig. 3B. A pair of sharp oxidation/reduction peaks of ferricyanide ion was detected at +328 and +256 mV with the ideally reversible redox behavior, as indicated by the separation of peak potentials (ΔE_p) of 72 mV. Another pair of intensive peaks was detected between +0.7 V and +0.8 V,

and was attributed to the redox reaction of electrodeposited CuO, whose standard redox potential is +0.747 V [31]. The following redox scheme for CuO is suggested [32]:



In case of reversible, diffusion-controlled process, the electroactive SA of an electrode can be predicted from Randles–Sevcik equation [33]:

$$I_p = 2.69 \times 10^5 A D^{1/2} n^{3/2} v^{1/2} C$$

where I_p represents peak current, A is an area of electrode (cm^2), n is the number of e^- participating in redox process (in our case $n = 1$), D represents diffusion coefficient of species in a solution, in our case $D = 6.70 \pm 0.02 \times 10^{-6} \text{ cm}^2 \text{ s}^{-1}$, C is the concentration of ferricyanide ion (5 mM) and v is the scan rate (50 mV s^{-1}). Taking into account all above data, the electroactive SA of CuO NWs modified GC electrode was estimated to 0.195 cm^2 .

3.2.2. The optimization of experimental conditions for the preparation of CuO NW/GC electrode

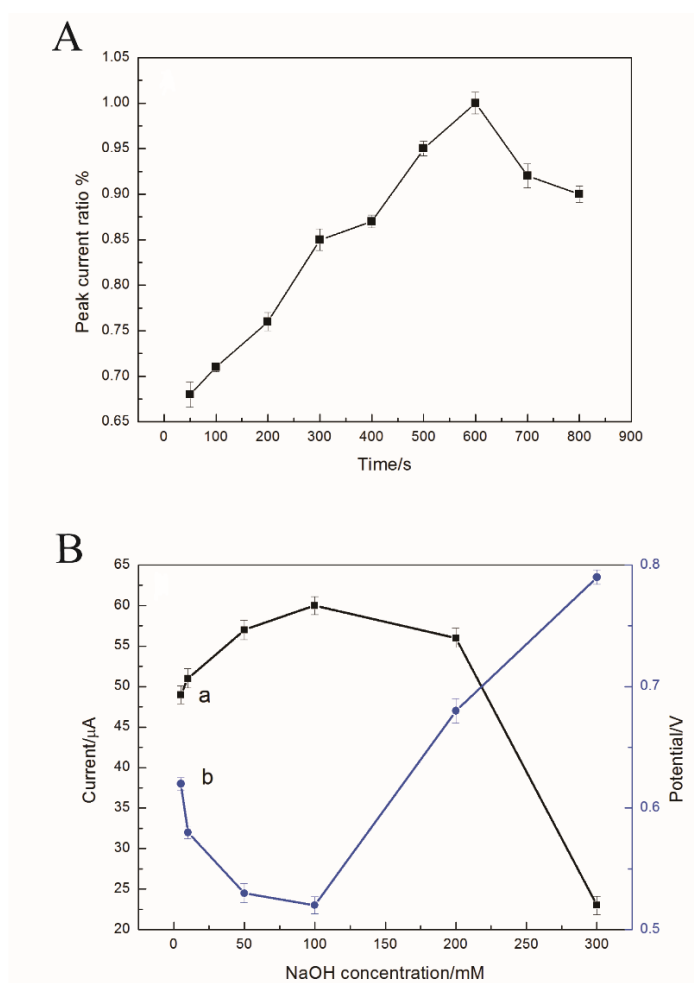


Figure 4. (A) The effect of electrodeposition time on the peak current ratio (I/I_{max}) towards 1mM Glc in 0.1M NaOH (B) The influence of NaOH concentration on the amperometric response (a) and peak potential (b) of the CuO NWs/GC electrode towards 1mM Glc.

In order to obtain the non-enzymatic Glc sensor with good sensitivity and wide linear detection range, we initially optimized electrodeposition time of Cu. Fig. 4A shows the effect of Cu electrodeposition time on the subsequent electrocatalytic activity of CuO NWs material in a Glc oxidation reaction. The current intensity increased with the deposition time, reaching the maximum value at 600 s and decreasing afterward. In the early stage of electrodeposition, the surface of electrode was not fully covered by Cu nanoparticles, resulting in less number of active sites for Glc electrocatalysis. The optimal number of active sites was reached after 600 s, while further deposition lead to excessive amount of Cu nanoparticles which were gathered too much, causing the reduction of the number of active sites.

Since catalytic oxidation of Glc involves hydroxide ions (see the reaction mechanism in Fig. 5.), the potential of oxidation and a corresponding peak current in CV are highly pH-dependent. The influence of pH on the oxidation of Glc at CuO NWs/GC was studied in a range of solutions containing various NaOH content (Fig. 4B). The peak current increased with the increase of NaOH concentration up to 100 mM, while higher amounts decreased signal intensity. At the same time, the peak potential shifted toward more negative values with the increase of NaOH concentration up to 100 mM. Therefore, the optimum experimental conditions for the synthesis of CuO NWs/GC electrode with superior catalytic performance toward Glc are 600 s for electrodeposition time and 100 mM for NaOH concentration.

3.2.3. Electrocatalytic oxidation of Glc at the CuO NWs/GC

To investigate the electrocatalytic activity of CuO NWs/GC electrode, CV were recorded in 40 mL 0.1 M NaOH in the presence or absence of Glc. Fig. 5A displays the CVs of pure GC and modified GC electrode without Glc in a solution. A wide reduction peak observed at +0.6 V (vs. Ag/AgCl) for two modified GC electrodes (Fig. 5A (a) and (b)) most likely originates from the reduction of Cu(III) to Cu(II) [34-35]. The corresponding oxidation peak, expected between +0.2 and +0.7 V was not clearly observed for both electrodes. The probable reason for this is the overlap with the oxidation peak for water [36]. Compared with Cu nanoparticles modified electrode (Fig. 5A(b)), CuO NWs/GC electrode exhibited higher oxidation and a broader reduction peak of water splitting (Fig. 5A(a)) as a result of larger SA and numerous electrocatalytic active sites.

The addition of Glc into 0.1 M NaOH induced the appearance of oxidation peaks in CV of CuO NW/GC electrode (Fig. 5B). The oxidation peak at +0.55 V gradually increased with the rise in Glc concentration from 1 to 9 mM. All these results imply the applicability of CuO for electrocatalytic oxidation of Glc. The possible mechanism for Glc oxidation on Cu-based catalysts in alkaline solution, first suggested by Marioli and Kuwana [37], can be represented by the following equations:



The oxidation peak observed in CVs at ~ 0.55 V confirms the oxidation of CuO to CuOOH in an alkaline medium (Eq. (1)) [38]. The generated CuOOH serves as an oxidation species for the conversion of Glc to gluconolactone (Eq. (2)) [39]. Afterward, gluconolactone is easily converted to gluconic acid

(Eq. (3)). In summary, Glc oxidation at CuO NWs in alkaline medium highly depends on the oxidation of Cu (II) to Cu (III) species.

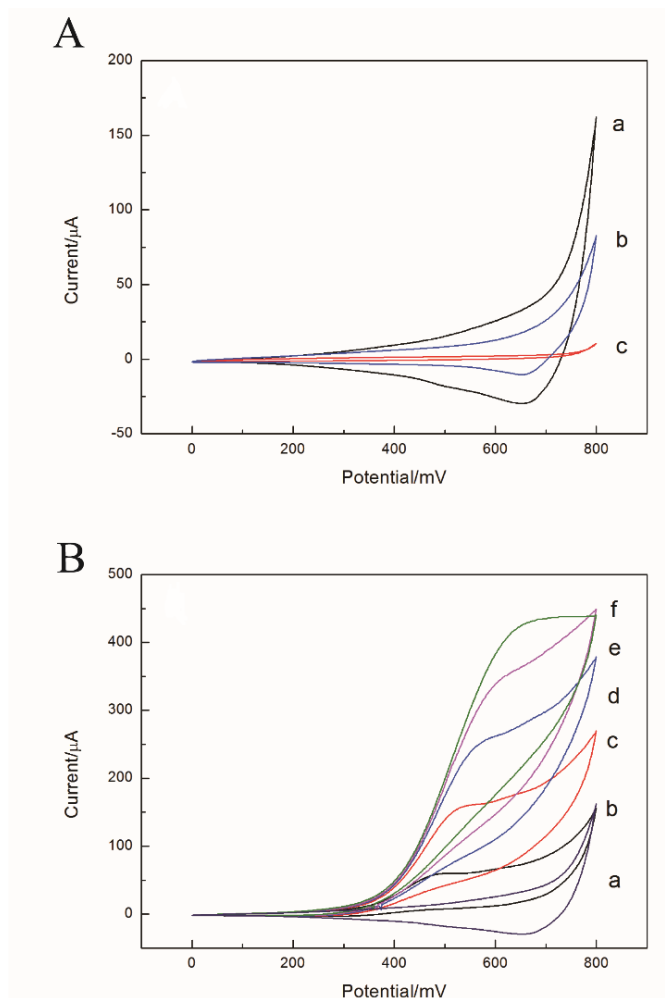


Figure 5. (A) CVs of CuO NWs/GC (a), Cu/GC (b) and pure GC electrode (c); (B) CVs of CuO NWs/GC electrode with various Glc concentration (from the bottom up: 0, 1, 3, 5, 7, and 9 mM). All measurements were performed in 0.1 M NaOH with 50 mV s^{-1} scan rate.

The amperometric response of CuO NWs/GC electrode under the applied potential of 0.55 V was recorded after successive addition of Glc (Fig. 6A). The gradual increase of oxidation current was observed, and 95% of equilibrium current intensity was reached within 4 s. As can be seen from calibration curve, the linear amperometric response was observed for Glc concentration range from 12.5 μM to 4.29 mM (Fig. 6B). The sensitivity of developed Glc sensor was $759.86 \mu\text{A mM}^{-1} \text{ cm}^{-2}$, calculated from the slope of linear calibration graph. The corresponding LOD was 4.17 μM , calculated from S/N ratio of 3. The comparison of sensor developed in this study with other nonenzymatic Glc sensors by means of linear range, LOD and sensitivity is summarized in Table 1. The superior characteristics of CuO NW/GC sensor may be explained by exceptionally large SA with large number of active sites capable for electrocatalytic oxidation of Glc.

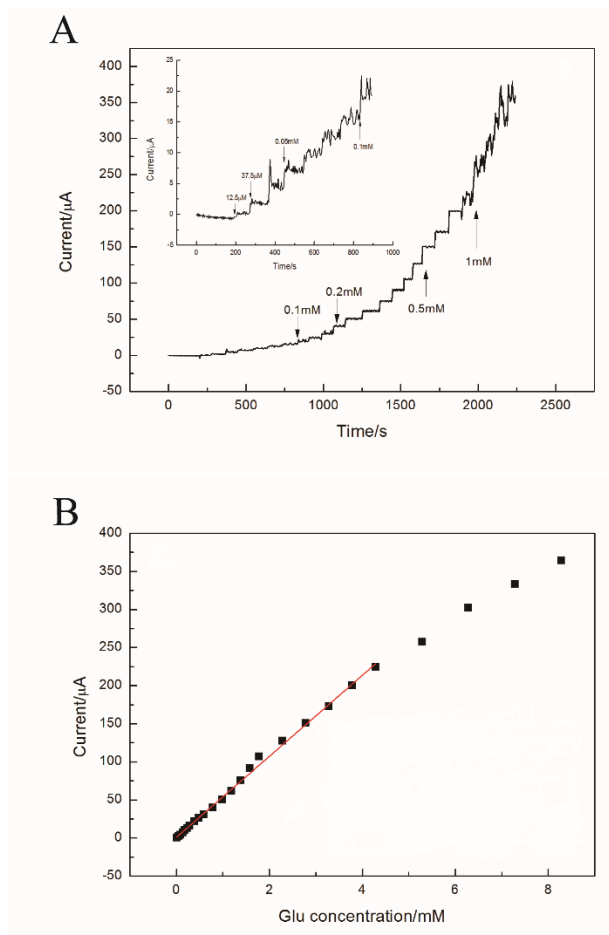


Figure 6. (A) Amperometric response of CuO NWs/GC electrode in a stirring 0.1 M NaOH containing the increasing amount of Glc. Inset: Magnified current-time responses at the lower concentration of Glc. (B) The corresponding Glc calibration curve.

Table 1. The performance of various non-enzymatic Glc sensors.

| Electrode | Applied potential (mV) | Linear range (up to mM) | LOD(μM) | Sensitivity (μA mM ⁻¹ cm ⁻²) | Reference |
|------------------------------|------------------------|-------------------------|---------|---|-----------|
| Cu ₂ O/graphene | 0.6 | 3.3 | 3.3 | 285 | [40] |
| Nafion/CuO nanospheres | 0.6 | 2.55 | N/A | 404.5 | [41] |
| CuO/CeO ₂ | 0.4 | 10 | 10 | 2.77 | [42] |
| SWNTs | 0.6 | 2.16 | 10 | 248.6 | [43] |
| Ag ₂ O nanowalls | 0.4 | 3.2 | 10 | 298.2 | [44] |
| NiO-SWNT | 0.5 | 1 | 0.3 | 907 | [45] |
| Ni(OH) ₂ nanoboxs | 0.58 | 5 | 0.07 | 487.3 | [46] |
| PVA/MnO ₂ @GO/CuO | 0.4 | 4.4 | 53 | N/A | [47] |
| CuO microflowers/nafion | 0.5 | 0.12 | 6.48 | 3100 | [18] |
| Nafion/RGO-Au NCs@CuO | 0.31 | 3 | 0.03 | N/A | [5] |
| CuO nanowires | 0.55 | 4.29 | 4.17 | 759.86 | This work |

3.2.4. Selectivity, reproducibility and stability of CuO NWs/GC electrode

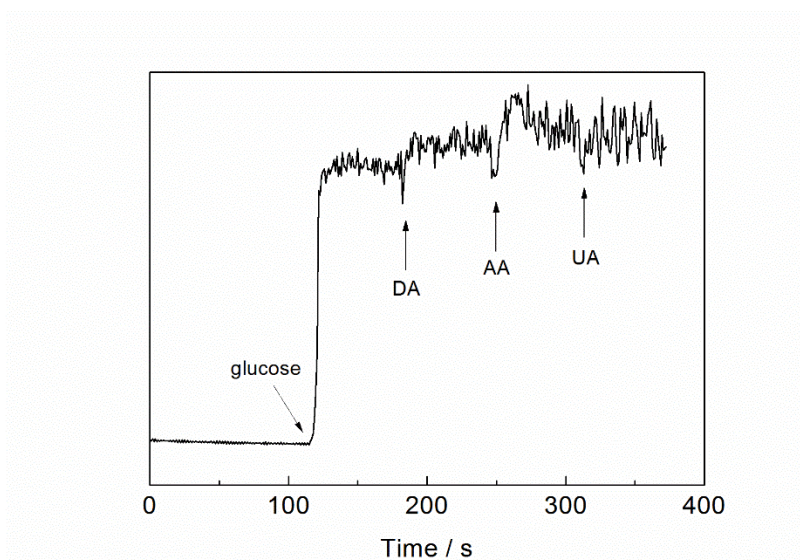


Figure 7. Interference test of CuO NWs/GC electrode in 0.1M NaOH solution containing 1 mM Glc and 0.1 mM DA, 0.1 mM AA, 0.5 mM UA as interfering compounds.

In the real samples, several electroactive substances such as DA, AA and UA might be present along with Glc analyte and interfere with the analytical signal. For the amperometric interference test, the concentrations of DA, AA and UA normally present in human blood (0.1 mM for DA and AA and 0.5 mM for UA) were studied. To quantify the selectivity and the influence of interfering species, amperometric responses of analyte (1 mM Glc) and other electroactive species were recorded at 0.55 V and compared. As can be seen from Fig. 7, the CuO NWs/GC is highly selective for Glc in the presence of DA, AA and UA, as their addition caused negligible change in the amperometric response of Glc analyte.

Besides selectivity and low interference with other substances from real samples, the reproducibility and stability are equally important characteristics of sensors. The device-to-device reproducibility was evaluated from the response to 1 mM glucose at five CuO NWs/GC electrodes independently, and the relative standard deviation was calculated to 4.16%. The monitoring of the analytical signal of CuO NWs/GC electrode toward 1 mM Glc solution for two weeks revealed an acceptable long-term stability, maintaining 89% of the initial current response.

3.2.5. Applications in real samples

The feasibility of the CuO NWs/GC sensing system for real samples was conducted in human blood serum through recovery experiments as presented in Table 2. After diluted to the specific concentration with 0.1 M PBS (pH 7.0), the recoveries of glucose detection in serums were determined range from 96%, 101% and 98%, respectively, indicating that this sensor shows potential applicability to real samples analysis.

Table 2. CuO NWs/GC electrode applied in real sample.

| Samples | Determination (mM) | Glc added (mM) | Glc found (mM) | Recovery (%) | RSD (%, n=6) |
|---------|-----------------------|-------------------|-------------------|-----------------|-----------------|
| 1 | 1.22 ± 0.5 | 5 | 5.98 ± 0.7 | 96 | 3.9 |
| 2 | 1.98 ± 0.8 | 10 | 12.12 ± 1.5 | 101 | 5.1 |
| 3 | 2.57 ± 1.1 | 15 | 17.2 ± 1.8 | 98 | 3.2 |

4. CONCLUSIONS

In summary, wirelike CuO nanostructures were efficiently produced by template- and surfactant-free electrodeposition technique. Owing to the large surface area, the nanowired CuO catalyst favorably oxidized Glc at the surface of modified GC electrode. Such sensor also exhibited high sensitivity, rapid response, and a broad linear range with a low LOD and acceptable reproducibility when applied for the quantification of Glc. The developed sensor provided the efficient monitoring of Glc at low potential (0.55 V vs. Ag/AgCl) where interference with common analytes from real samples such as dopamine, ascorbic and uric acid was negligible. The results presented in this study highlight the potential of CuO nanowire structures for fabrication of non-enzymatic Glc sensors. The electrodeposition proved to be a simple, rapid and controllable method for fabricating wirelike electrocatalysts which might be applied for the production of similar nanomaterials from other noble metals.

ACKNOWLEDGEMENT

The financial supports from National Natural Science Foundation of China (Grant Nos. 81973944 and 81503636) and Tianjin Natural Science Foundation (Grant No. 16JCQNJC12400) are acknowledged.

References

1. S. Fu, G. Fan, L. Yang and F. Li, *Electrochim. Acta*, 152 (2015) 146.
2. S.A. Zaidi and J.H. Shin, *Talanta*, 149 (2016) 30.
3. N. Zhang, T. Wilkop, S. Lee and Q. Cheng, *Analyst*, 132 (2007) 164.
4. M. Kirthiga, L. Rajendran and C. Fernandez, *Electrochim. Acta*, 230 (2017) 89.
5. Q. Liu, Z. Jiang, Y. Tang, X. Yang, M. Wei and M. Zhang, *Sens. Actuators B: Chem.*, 255 (2017) 454.
6. A.E. Cass, G. Davis, G.D. Francis, H.A. Hill, W.J. Aston, I.J. Higgins, E.V. Plotkin, L.D. Scott and A.P. Turner, *Anal. Chem.*, 56 (1984) 667.
7. Z. Fan, B. Liu, X. Liu, Z. Li, H. Wang, S. Yang and J. Wang, *Electrochim. Acta*, 109 (2013) 602.
8. C. Zhang, Y. Zhang, X. Du, Y. Chen, W. Dong, B. Han and Q. Chen, *Talanta*, 159 (2016) 280.
9. M. Baghayeri, A. Amiri and S. Farhadi, *Sens. Actuators B: Chem.*, 225 (2016) 354.
10. Y. Fang, D. Zhang, Y. Guo, Y. Guo and Q. Chen, *Sens. Actuators B: Chem.*, 221 (2015) 265.

11. X. Kang, Z. Mai, X. Zou, P. Cai and J. Mo, *Anal. Biochem.*, 363 (2007) 143.
12. Z. Zhuang, X. Su, H. Yuan, Q. Sun, D. Xiao and M.M. Choi, *Analyst*, 133 (2007) 126.
13. K. Li, G. Fan, L. Yang and F. Li, *Sens. Actuators B: Chem.*, 199 (2014) 175.
14. L. Tang, J. Lv, C. Kong, Z. Yang and J. Li, *New J. Chem.*, 40 (2016) 6573.
15. L. Lin, B.B. Karakocak, S. Kavadiya, T. Soundappan and P. Biswas, *Sens. Actuators B: Chem.*, 259 (2018) 745.
16. Y. Tian, Y. Liu, W.P. Wang, X. Zhang and W. Peng, *Electrochim. Acta*, 156 (2015) 244.
17. L. Tian and B. Liu, *Appl. Surf. Sci.*, 283 (2013) 947.
18. V. Vinoth, T.D. Shergilin, A.M. Asiri, J.J. Wu and S. Anandan, *Mat. Sci. Semicon. Proc.*, 82 (2018) 31.
19. L. Luo, L. Zhu and Z. Wang, *Bioelectrochemistry*, 88 (2012) 156.
20. X. Wang, C. Ge, K. Chen and Y.X. Zhang, *Electrochim. Acta*, 259 (2018) 225.
21. J. Yang, Q. Lin, W. Yin, T. Jiang, D. Zhao and L. Jiang, *Sens. Actuators B: Chem.*, 253 (2017) 1087.
22. R. Yuan, H. Li, X. Yin, J. Lu and L. Zhang, *Talanta*, 174 (2017) 514.
23. Y. Sun, B. Mayers, A. Thurston Herricks and Y. Xia, *Nano Lett.*, 3 (2003) 955.
24. S. Radhakrishnan, H.Y. Kim and B.S. Kim, *Sens. Actuators B: Chem.*, 233 (2016) 93.
25. M. Kuang, T.T. Li, H. Chen, S.M. Zhang, L.L. Zhang and Y.X. Zhang, *Nanotechnology*, 26 (2015) 304002.
26. W.H. Antink, Y. Choi, K. Seong and Y. Piao, *Sens. Actuators B: Chem.*, 255 (2018) 1995.
27. J. Zhu, W. Nie, Q. Wang, J. Li, H. Li, W. Wen, T. Bao, H. Xiong, X. Zhang and S. Wang, *Carbon*, 129 (2018) 29.
28. J.S. Shaikh, R.C. Pawar, A.V. Moholkar, J.H. Kim and P.S. Patil, *Appl. Surf. Sci.*, 257 (2011) 4389.
29. D.P. Dubal, G.S. Gund, R. Holze and C.D. Lokhande, *J. Power Sources*, 242 (2013) 687.
30. L.W. Zhi and L.Y. Qin, *Sens. Actuators B: Chem.*, 141 (2009) 147.
31. J. Yang, L. Jiang, W. Zhang and S. Gunasekaran, *Talanta*, 82 (2010) 25.
32. D. Zoubov, Nina, Atlas d'equilibres electrochimiques, Gauthier-Villars, 1963.
33. A.J. Bard and L.R. Faulkner, *J. Chem. Educ.*, 1 (2001) 669.
34. Z. Chen, B. Zhao, X. Fu, R. Sun and C. Wong, *J. Electroanal. Chem.*, 807 (2017) 220.
35. S. Luo, F. Su, C. Liu, J. Li, R. Liu, Y. Xiao, Y. Li, X. Liu and Q. Cai, *Talanta*, 86 (2011) 157.
36. L.C. Jiang and W.D. Zhang, *Biosens. Bioelectron.*, 25 (2010) 1402.
37. J.M. Marioli and T. Kuwana, *Electrochim. Acta*, 37 (1992) 1187.
38. T. Alizadeh and S. Mirzagholidpur, *Sens. Actuators B: Chem.*, 198 (2014) 438.
39. S. Sun, X. Zhang, Y. Sun, S. Yang, X. Song and Z. Yang, *Chem. Phys.*, 15 (2013) 10904.
40. M. Liu, R. Liu and W. Chen, *Biosens. Bioelectron.*, 45 (2013) 206.
41. E. Reitz, W. Jia, M. Gentile, Y. Wang and Y. Lei, *Electroanal.*, 20 (2010) 2482.
42. P. Guan, Y. Li, J. Zhang and W. Li, *Nanomaterials*, 6 (2016) 159.
43. J. Wang, X. Sun, X. Cai, Y. Lei, L. Song and S.S. Xie, *Electrochim. Solid St.*, 10 (2007) 58.
44. B. Fang, A. Gu, G. Wang, W. Wang, Y. Feng, C. Zhang and X. Zhang, *ACS Appl. Mater. Inter.*, 1 (2009) 2829.
45. N.Q. Dung, D. Patil, H. Jung, J. Kim and D. Kim, *Sens. Actuators B: Chem.*, 183 (2013) 381.
46. J. Nai, S. Wang, Y. Bai and L. Guo, *Small*, 9 (2013) 3147.
47. M.M. Farid, L. Goudini, F. Piri, A. Zamani and F. Saadati, *Food Chem.*, 194 (2016) 61.